Eur. Phys. J. A **19**, 173–185 (2004)
DOI 10.1140/epja/i2003-10120-5

THE EUROPEAN PHYSICAL JOURNAL A

Coexisting wobbling and quasiparticle excitations in the triaxial potential well of ^{163}Lu

D.R. Jensen[1], G.B. Hagemann[1,a], I. Hamamoto[1,2], B. Herskind[1], G. Sletten[1], J.N. Wilson[1], S.W. Ødegård[3], K. Spohr[4], H. Hübel[5], P. Bringel[5], A. Neußer[5], G. Schönwaßer[5], A.K. Singh[5], W.C. Ma[6], H. Amro[6,b], A. Bracco[7], S. Leoni[7], G. Benzoni[7], A. Maj[8], C.M. Petrache[9,10], G. Lo Bianco[10], P. Bednarczyk[8,11], and D. Curien[11]

[1] The Niels Bohr Institute, Blegdamsvej 17, DK-2100 Copenhagen Ø, Denmark
[2] Department of Mathematical Physics, LTH, University of Lund, Lund, Sweden
[3] Department of Physics, University of Oslo, PB 1048 Blindern, N-0316 Oslo, Norway
[4] Department of Electronic Engineering and Physics, University of Paisley, Scotland, UK
[5] Helmholtz-Institut für Strahlen- und Kernphysik, University of Bonn, Nußallee 14-16, D-53115 Bonn, Germany
[6] Mississippi State University, Mississippi State, MS 39762, USA
[7] Dipartimento di Fisica and INFN, Sezione di Milano, Milano, Italy
[8] Niewodniczanski Insitute of Nuclear Physics, Krakow, Poland
[9] Dipartimento di Fisica and INFN, Sezione di Padova, Padova, Italy
[10] Dipartimento di Matematica e Fisica, Università di Camerino, Camerino, Italy
[11] IReS, 23 rue du Loess, BP28 F-67037, Strasbourg, France

Received: 18 July 2003 / Revised version: 28 August 2003 /
Published online: 23 December 2003 –
Communicated by D. Schwalm

Abstract. High-spin states of the nucleus ^{163}Lu have been populated through the fusion-evaporation reaction ^{139}La(^{29}Si, $5n$) with a beam energy of 157 MeV. In addition to the two lowest excited triaxial strongly deformed (TSD) bands, recently interpreted as one- and two-phonon wobbling excitations, a third excited TSD band has been firmly established decaying to the yrast TSD band. The assignment of this band as a three-quasiparticle band shows together with the normal deformed (ND) level scheme the presence not only of shape coexistence between ND and TSD structures, but also an interplay of wobbling and quasiparticle excitations in the triaxial strongly deformed potential well of ^{163}Lu.

PACS. 21.10.-k Properties of nuclei; nuclear energy levels – 23.20.Lv γ transitions and level energies – 25.70.-z Low and intermediate energy heavy-ion reactions – 27.70.+q $150 \leq A \leq 189$

1 Introduction

Nuclei in the mass region around $A \sim 165$ have been predicted to possess stable triaxial strongly deformed (TSD) shapes at higher rotational frequency [1,2]. In total potential energy surfaces of Lu and Hf nuclei in this mass region, calculated using the Ultimate Cranker (UC) code [3,4], well-developed local TSD minima with $(\epsilon, \gamma) \sim (0.40, \pm 20^\circ)$ appear for all combinations of parity and signature (π, α). The TSD minima are predicted to coexist with the global normal deformed (ND) minimum at $(\epsilon, \gamma) \sim (0.22, 0^\circ)$.

Experimentally more than 30 TSD bands have been observed in the $A \sim 165$ mass region in Lu and Hf isotopes [5]. Quadrupole moments confirming the large deformation related to these rotational structures have been measured in lifetime experiments for ^{163,164,165}Lu [6–9] and ^{168}Hf [10]. Recently, the first evidence for the triaxial deformation of nuclei belonging to the $A \sim 165$ mass region has been provided by the observation of a one-, and a two-phonon wobbling excitation in ^{163}Lu [11,12]. The wobbling mode is uniquely related to the triaxiality of the nuclear system. Very recently a one-phonon wobbling excitation has been found in both ^{165}Lu [13] and ^{167}Lu [14], and possibly also in ^{161}Lu [15]. In ^{165}Lu even a two-phonon wobbling band is most likely identified as well with a very close resemblance to the counterpart in ^{163}Lu [13]. These observations establish the wobbling mode as a more general phenomenon in the $A \sim 165$ region.

The triaxial deformation of a nuclear system allows for collective rotation about any of the principal axes of the nuclear shape. Therefore, triaxial nuclei are expected

[a] e-mail: hagemann@nbi.dk
[b] *Present address*: Wright Nuclear Structure Laboratory, Yale University, New Haven, CT 06520-8124, USA.

to show more rich rotational spectra compared to axially symmetric deformed nuclei. This expectation has been verified by the observation of wobbling phonon excitations, a mode where some of the collective angular momentum is transferred to the two axes with smaller moments of inertia. The wobbling interpretations in ^{161,163,165,167}Lu are based on a comparison with particle-rotor calculations in which an aligned high-j proton is coupled to a triaxial core [16,17]. However, the possibility of rotational bands of which the intrinsic structure can be understood in terms of quasiparticle excitations, should still exist. Such excitations may be investigated by principal axis cranking calculations.

In the present paper we focus on a fourth TSD band, TSD4, which has been observed in ^{163}Lu in addition to the lower-lying bands, TSD2 and TSD3, assigned as one- and two-phonon wobbling excitations, respectively. TSD4, reported for the first time in ref. [18], is observed to decay to the yrast $\pi i_{13/2}$ band, TSD1, through four firmly established decay-out transitions. The assignment of TSD2 and TSD3 as wobbling excitations built on TSD1 was based partly on the observation of very similar rotational properties of these three bands, reflecting a similarity in the intrinsic structure which is expected for a sequence of wobbling bands [11,12]. However, TSD4 exhibits rotational properties quite different from those of TSD1-3. In the following, we investigate the different possibilities for assigning TSD4 as a three-quasiparticle excitation based on a comparison with UC calculations.

In the present experiment the normal deformed level scheme of ^{163}Lu has been extended compared to the one published in ref. [18]. New bands have been observed and configurations will be proposed in the following.

2 Experiment

In a dedicated search for a second-phonon wobbling excitation high-spin states of the nucleus ^{163}Lu were populated by the fusion-evaporation reaction ^{139}La(^{29}Si, $5n$) with a beam energy of 157 MeV provided by the Vivitron accelerator at IReS, Strasbourg [12]. The thickness of the self-supporting La target was 500 μg/cm^2. In ten days of beam time $6 \cdot 10^9$ events were collected with the Euroball detector array with 3 or more Compton suppressed γ-rays in the Ge detectors and 8 or more γ-rays in the BGO inner ball. At the time of the experiment, Euroball consisted of 15 Cluster, 25 Clover and 27 Tapered operational Ge detectors [19].

2.1 Sorting of the data

The data were sorted into a data base on disk from which one Radware 3D coincidence cube [20] was made for further coincidence analysis. One 2D matrix was sorted using the so-called filtering technique [21], where a filter spectrum containing transitions from the yrast TSD band, TSD1, was applied. For the spin and parity determination of rotational bands a number of 2D matrices were sorted with different detector angle combinations along the axes to be used in the angular distribution and DCO (Directional Correlation from Oriented states) ratio analysis. For the angular distribution analysis two matrices with the axis combinations (all detectors $\times$ detectors at 25°) and (all detectors $\times$ detectors at 90°) were made. The detectors comprising those at 25° were the 5 detectors in the most inner ring of the two Cluster rings in the backward direction, and the 15 detectors situated in the inner and middle rings of the three Tapered rings in the forward direction of the Euroball array. The 90° data were collected using all the Clover detectors. A matrix with the angle combination (detectors at 90° $\times$ detectors at 25°) was made for the DCO analysis. In order to determine the spin-alignment (σ/I), see sect. 3, a fourth matrix with (detectors at 25° $\times$ detectors at 25°) was needed. Linear polarization measurements were obtained based on data detected at 90° in the Clover detectors by separating the γ-rays scattered horizontally from those scattered vertically in the four crystals of each detector. For this analysis the data were sorted into two matrices with (all detectors $\times$ vertical) and (all detectors $\times$ horizontal), respectively.

3 Spin and parity determination

The multipolarity of the decay-out transitions of the various bands was determined from an angular distribution and DCO ratio analysis. The spin alignment, experimentally extracted as σ/I, for a Gaussian distribution of the m-substate population, $P_m(I) \propto \exp(-\frac{m^2}{2\sigma(I)^2})$ with half-width σ, was obtained in a detector efficiency independent way. For a more detailed description of this method see ref. [18]. An average of $\sigma/I = 0.25 \pm 0.02$ was measured for transitions within the yrast TSD band, TSD1, in the spin range from $29/2\hbar$ to $61/2\hbar$. No spin dependence of σ/I was detectable in the spin interval considered. The

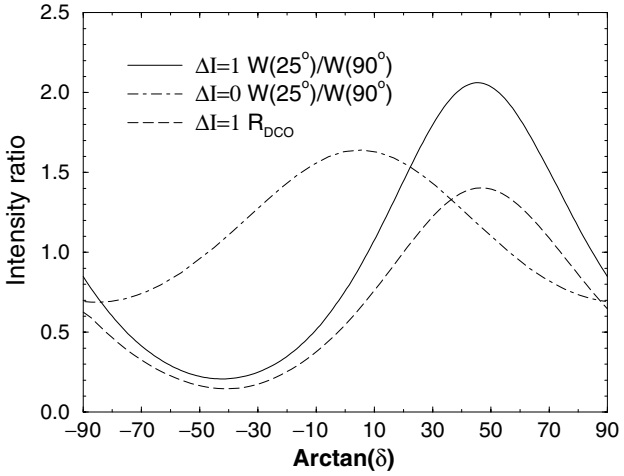

Fig. 1. Calculated angular distribution and DCO ratios as a function of the mixing ratio, δ.

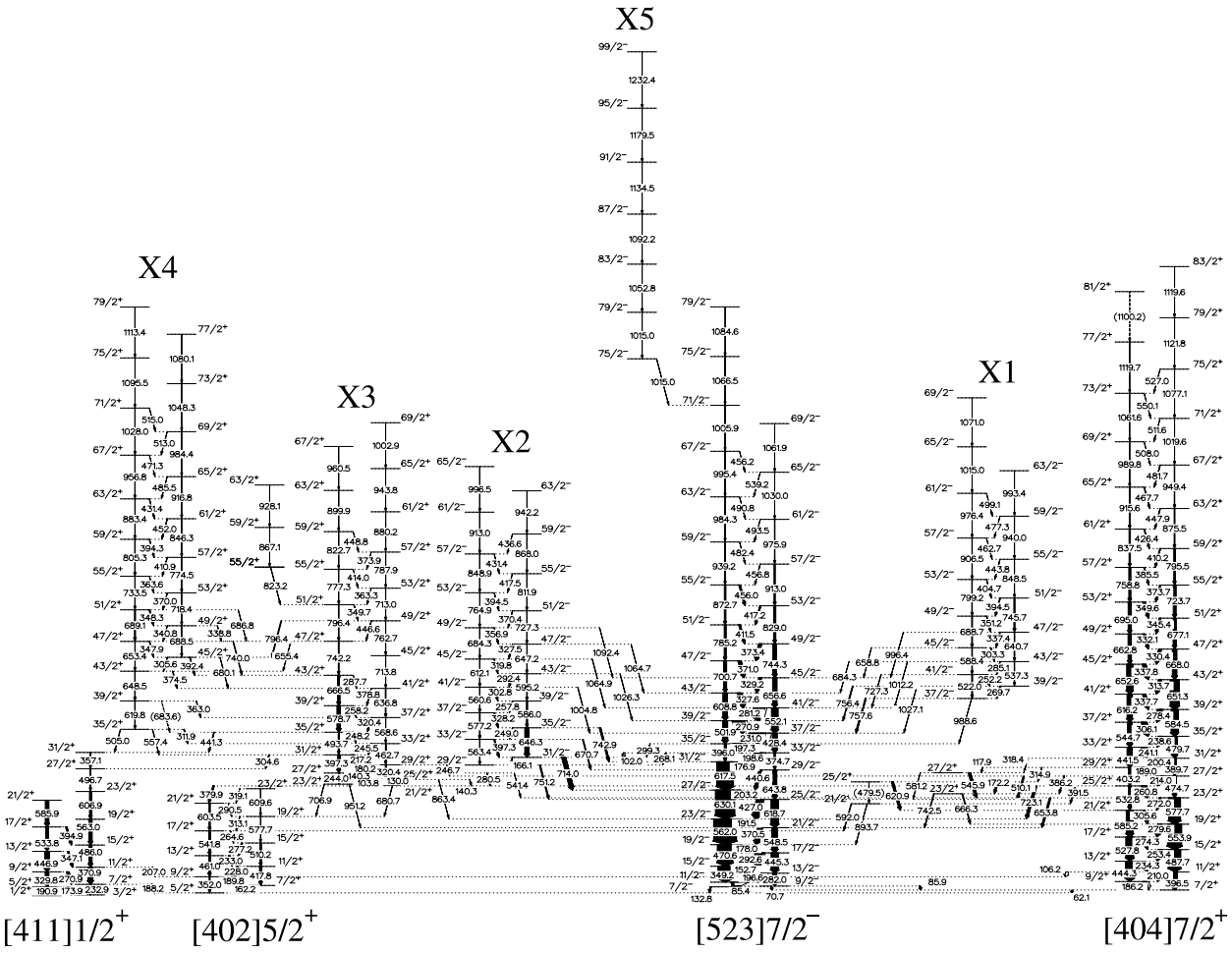

Fig. 2. Level scheme of observed normal deformed structures in ^{163}Lu.

DCO ratio, $R_{\rm DCO}$, is defined as

$$R_{\rm DCO} = \frac{I^{\gamma_1}_{25^\circ}(\mathrm{Gate}^{\gamma_2}_{90^\circ})}{I^{\gamma_1}_{90^\circ}(\mathrm{Gate}^{\gamma_2}_{25^\circ})}, \qquad (1)$$

where $I^{\gamma_1}_{25^\circ}(\mathrm{Gate}^{\gamma_2}_{90^\circ})$ represents the intensity of a transition γ_1, determined from a spectrum obtained with a detector at 25°, gated on the transition γ_2 in a detector situated at 90°. DCO ratios were obtained experimentally using the matrix with (detectors at 90° × detectors at 25°). The angular distribution ratio, $W(25°)/W(90°)$, was measured using the two matrices sorted with (all detectors × detectors at 25°) and (all detectors × detectors at 90°). In fig. 1 calculated $W(25°)/W(90°)$ ratios are shown as a function of the mixing ratio, δ, for $\Delta I = 0$ ($45/2\hbar \rightarrow 45/2\hbar$) and $\Delta I = 1$ ($45/2\hbar \rightarrow 43/2\hbar$) transitions using $\sigma/I = 0.25$. The calculated DCO ratio for the first $\Delta I = 1$ transition in a γ-cascade with spins $39/2\hbar \rightarrow 37/2\hbar \rightarrow 33/2\hbar$ gated on the last $\Delta I = 2$ transition is also shown in fig. 1. It should be noted that the spin dependence of both the DCO and angular distribution ratios is not very pronounced. Measurements of the polarization

$$P = \frac{(I_{\rm vertical} - I_{\rm horizontal})}{(I_{\rm vertical} + I_{\rm horizontal})} \qquad (2)$$

yielded an average value for known stretched $E2$ transitions of $P = +0.11 \pm 0.03$ and for known stretched $M1$ transitions $P = -0.11 \pm 0.05$.

4 Results

In fig. 2 the level scheme of normal deformed structures of ^{163}Lu is shown. A total of eight coupled bands and one single band has been observed compared to six coupled bands in the previous experiment [18]. Figure 3 shows the four triaxial strongly deformed bands together with the decay-out transitions to ND states.

4.1 Normal deformed structures

In ref. [18] a detailed discussion of the ND bands established in the previous experiment on ^{163}Lu can be found. In this section, configurations of the new ND structures observed in the present experiment will be discussed. The configurations have been assigned based on a comparison with UC calculations, which at lower spin predict bands built on the proton orbitals, [411]1/2$^+$, [402]5/2$^+$,

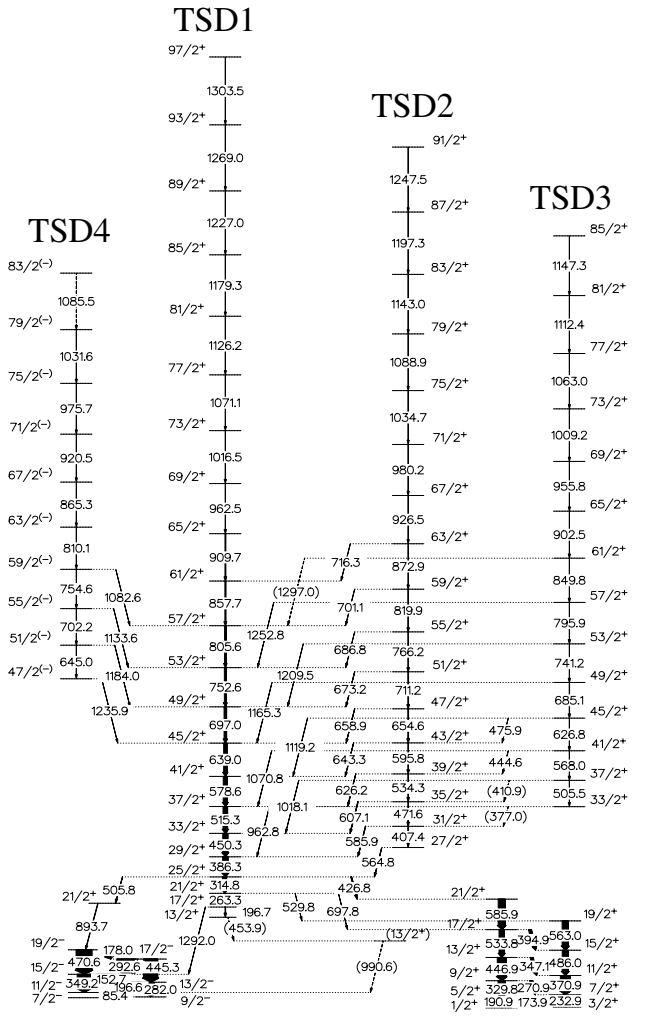

Fig. 3. Partial level scheme of ^{163}Lu showing the four firmly established TSD bands.

Table 1. Labelling of the lowest Nilsson orbitals for neutrons.

Nilsson orbital	$\alpha = +1/2$	$\alpha = -1/2$
$[642]5/2^+$	A	B
$[651]3/2^+$	C	D
$[523]5/2^-$	E	F
$[521]3/2^-$	G	H

$[404]7/2^+$, $[514]9/2^-$ and $[523]7/2^-$. At higher-spin configurations involving one of the lowest protons coupled to two low-lying quasineutrons are expected. The labelling of the Nilsson orbitals for neutrons and protons is shown in tables 1 and 2, respectively.

Many of the lowest bands predicted by UC have been established experimentally in the previous experiment [18]. In fig. 2 these bands are labelled with Nilsson quantum numbers at low spin. Two new coupled bands, X2 and X3, have been observed in the present experiment as well as one single band, X5. All the decay-out transitions of the previously known ND bands have been confirmed in the present experiment. Due to strong mixing between levels especially in the bands now labelled X3 and X4, some of the levels have been rearranged compared to ref. [18]. It should be noted that in ref. [18] the $[411]1/2^+$ band was extended to up to spin $59/2\hbar$, whereas in the present level scheme the $[411]1/2^+$ band ends at spin $31/2\hbar$. The top of $[411]1/2^+$ in ref. [18] now comprises a part of the new band X3 from spin $39/2\hbar$ to $51/2\hbar$ in addition to the short band with the three levels 55/2, 59/2 and $63/2\hbar$ decaying into X3 at spin $51/2\hbar$ through the 823.2 keV γ-ray. The top part of X3 from spin $45/2\hbar$ in the positive-signature partner and from spin $55/2\hbar$ in the negative-signature partner are new extensions. The lowest part of the band X3 was also seen in the previous experiment. Levels now placed in the positive-signature partner up to spin $41/2\hbar$ as well as the levels up to spin $31/2\hbar$ in the negative-signature partner belonged to the band labelled X2 in ref. [18]. In some of the other previously known bands smaller changes have been made at the highest spins and a few new transitions have been added.

Table 2. Labelling of the lowest Nilsson orbitals for protons.

Nilsson orbital	$\alpha = +1/2$	$\alpha = -1/2$
$[411]1/2^+$	a	b
$[404]7/2^+$	c	d
$[402]5/2^+$	k	l
$[523]7/2^-$	e	f
$[514]9/2^-$	g	h
$[660]1/2^+$	m	
$[541]1/2^-$	n	

In figs. 4 and 5 the excitation energy relative to a rigid-rotor reference of negative- and positive-parity ND bands, respectively, is shown, and for each band the proposed configuration is indicated. The alignment of the same bands is shown in figs. 6 and 7 as a function of rotational frequency using a reference $I_{\rm ref} = \mathcal{J}_0\omega + \mathcal{J}_1\omega^3$ with $J_0 = 30\hbar^2$ MeV^{-1} and $J_1 = 40\hbar^4$ MeV^{-3}.

4.1.1 The bands $[402]5/2^+$ and $[411]1/2^+$

The bands $[402]5/2^+$ and $[411]1/2^+$ were also observed in the previous experiment and the present data set confirms the earlier observations [18] and the configuration assignments of these bands.

4.1.2 The bands $[404]7/2^+$ and $[523]7/2^-$

In the $[404]7/2^+$ band the first neutron crossing, AB, is observed at $\hbar\omega \sim 0.26$ MeV, see fig. 7, and at $\hbar\omega \sim 0.32$ MeV another crossing occurs matching the frequency of the BC crossing. However, the BC crossing should be blocked after the AB alignment, and it was therefore proposed in ref. [18] that a change of character takes place in the $[404]7/2^+$ band into $[523]7/2^-\otimes$AEBC after the apparent AB crossing. That is, the two signature partners are built on the e and f protons, respectively, together with the quasineutrons AE going into AEBC at $\hbar\omega \sim 0.32$ MeV,

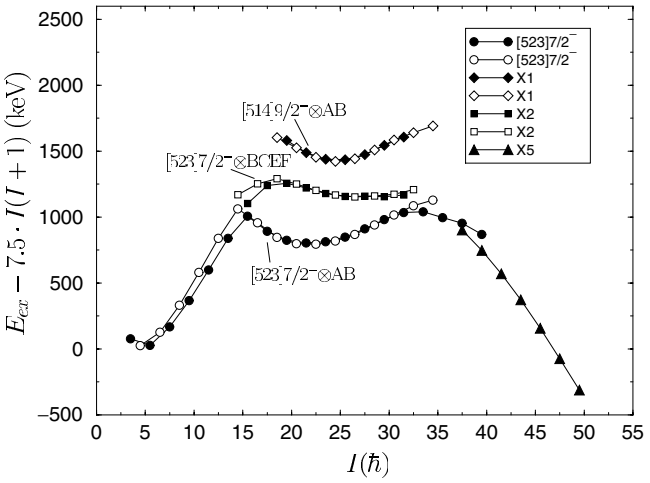

Fig. 4. Excitation energy as a function of spin for negative-parity ND bands relative to a rigid-rotor reference.

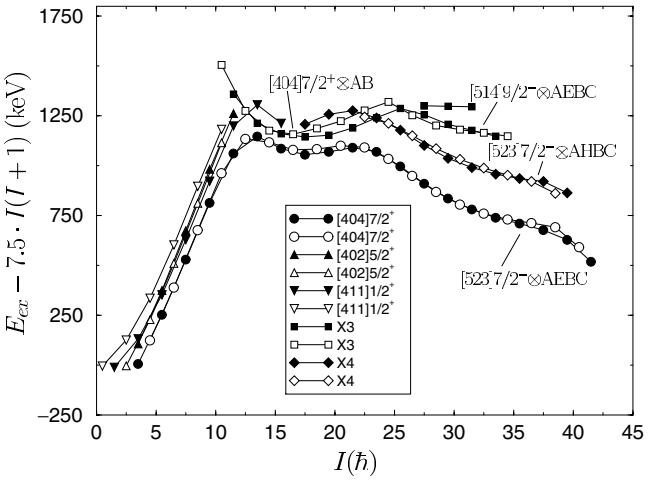

Fig. 5. Excitation energy as a function of spin for positive-parity ND bands relative to a rigid-rotor reference.

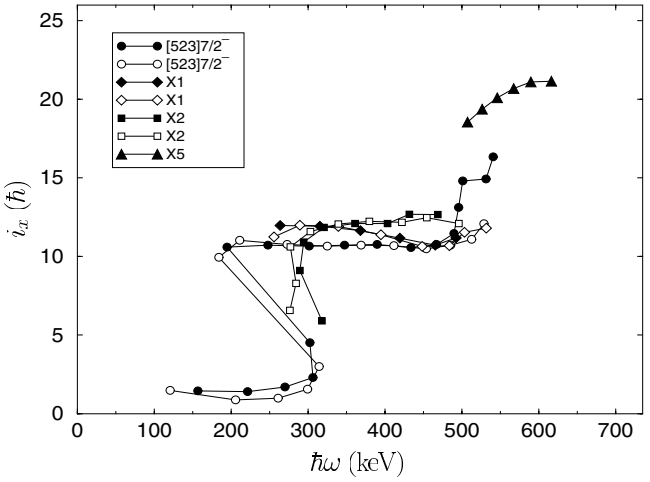

Fig. 6. Alignment as a function of rotational frequency for negative-parity ND bands.

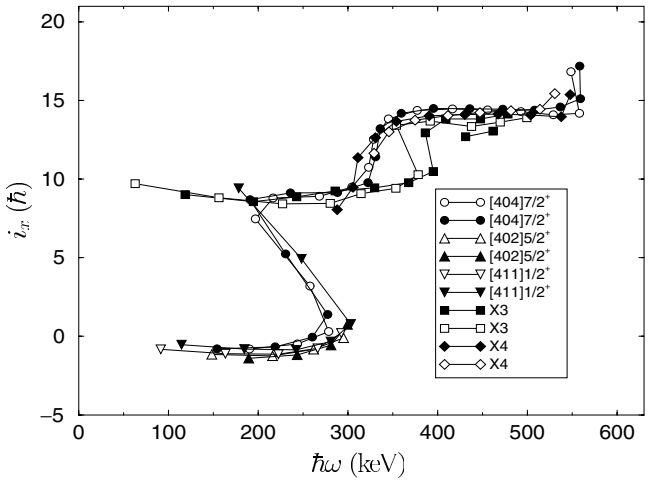

Fig. 7. Alignment as a function of rotational frequency for positive-parity ND bands.

see also sect. 4.1.5. At a frequency of $\sim$ 0.54 MeV the onset of a new alignment gain is seen probably caused by the second $h_{11/2}$ proton crossing.

The $[523]7/2^-$ band has a very constant alignment after the AB crossing at $\hbar\omega \sim 0.26$ MeV, fig. 6, up to $\hbar\omega \sim 0.5$ MeV, where an alignment gain is observed probably also due to the second $h_{11/2}$ proton crossing.

4.1.3 The band X1

In ref. [18] the spin and parity of this band were ambiguous and no configuration was proposed. However, due to the increased statistics in the present experiment angular distribution and DCO ratios have now been measured for some of the decay-out transitions as well as polarization, see table 3.

The band decays through five $\Delta I = 0$ and four $\Delta I = 1$ $M1$ transitions. The measured $W(25°)/W(90°)$ ratios for the 684.3, 727.3 and 757.6/756.4 keV γ-rays could also correspond to $\Delta I = 1$ mixed $E2/M1$ nature dominated by $M1$, see fig. 1. However, the 1012.2 keV transition would then be of $\Delta I = 2$ character disagreeing with the observed $W(25°)/W(90°)$ ratio for this transition for which the expected ratio is $\sim$ 1.5. Based on these results X1 was firmly assigned negative parity. With the proposed spin assignment, X1 has a rather high excitation energy, see fig. 4, and it is suggested that the configuration of this band could involve the next proton orbital $[514]9/2^-$. From the alignment plot, fig. 6, it is

Table 3. Angular distribution ratios, DCO ratios and polarization measurements of decay-out transitions from band X1.

E_γ (keV)	ΔI	$\frac{W(25°)}{W(90°)}$	$R_{\rm DCO}$	P
1012.2	1	1.03 ± 0.20	0.72 ± 0.20	
684.3	0	1.73 ± 0.35		
727.3	0	1.61 ± 0.31	0.99 ± 0.18	-0.22 ± 0.04
757.6/756.4	0	1.68 ± 0.34	1.22 ± 0.24	-0.12 ± 0.03

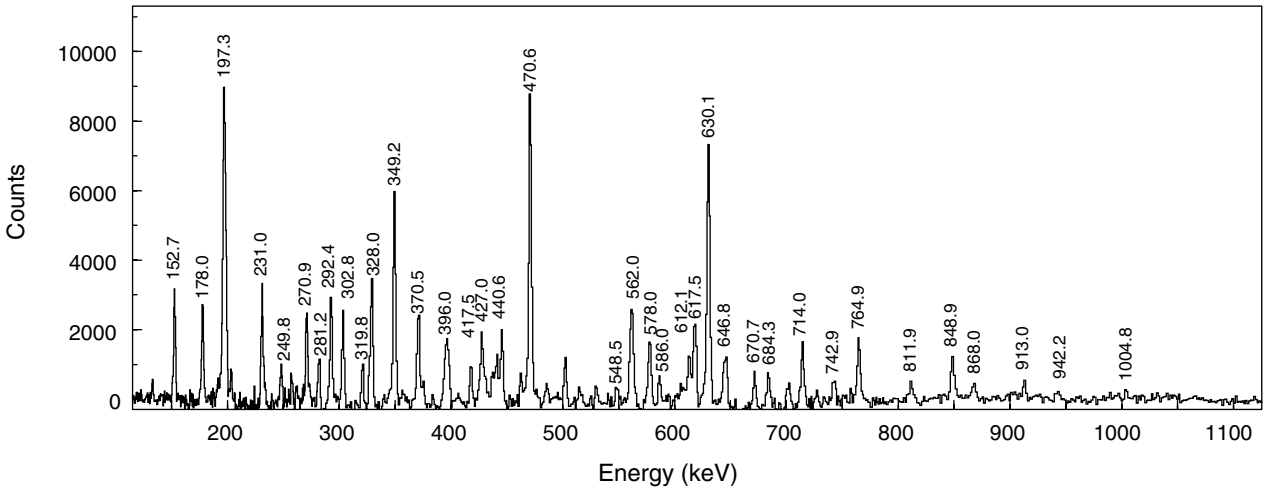

Fig. 8. Spectrum showing the ND band, X2, obtained from the 3D-coincidence cube using a sum of double gates on the transitions 560.6, 612.1 and 684.3 keV.

evident that the configuration contains the AB neutrons as well. It is therefore proposed that the configuration of X1 is $[514]9/2^-\otimes$AB. Furthermore, X1 shows the same behavior as the band $[523]7/2^-\otimes$AB, fig. 4, as a function of spin. The energy difference of ~ 600 keV at spin $67/2\hbar$ between the bands $[523]7/2^-\otimes$AB and X1 then represents the difference between the $[523]7/2^-$ and $[514]9/2^-$ orbitals, for which the calculated value is ~ 500 keV.

4.1.4 The band X2

The band X2 is observed for the first time in the present experiment and a spectrum is shown in fig. 8. Only the level with $I^\pi = 31/2^-$ was reported in ref. [18]. The spin is fixed due to several inter-band transitions between X2 and the $[523]7/2^-\otimes$AB band at spin $31/2^-$. Excluding the possibility for transitions of $M2$ nature negative parity has been assigned to X2. The band is mainly depopulated through a rather strong γ-ray of 714.0 keV to the $[523]7/2^-$ band. Several other $\Delta I = 2$ $E2$ transitions are found to decay to the $[523]7/2^-\otimes$AB band. From fig. 4 it appears that the band has an excitation energy a little higher than the $[523]7/2^-\otimes$AB band and it clearly looks like the continuation of the $[523]7/2^-$ band into $[523]7/2^-\otimes$BC. This interpretation agrees with the observed BC alignment at $\hbar\omega \sim 0.31$ MeV, fig. 6. However, at ~ 0.4 MeV the alignment is $\sim 2\hbar$ larger than that of the $[523]7/2^-\otimes$AB band, which suggests that other neutrons, for example EF or AD could be involved in the configuration as well.

4.1.5 The band X3

The band X3 is also new, see fig. 9. Four new $\Delta I = 1$ decay-out transitions of energies 140.3, 280.5, 246.7 and 541.4 keV have been found decaying from the lower part of the band to the $[404]7/2^+$ band. At spins around $45/2\hbar$ the $M1$ inter-band transitions are weak and not observed. At intermediate spins the band interacts with the band X4. Due to the many decay-out transitions of $\Delta I = 0, 1$ and 2 nature the spin of band X3 is fixed and negative parity has been assigned to this band by excluding the possibility for transitions of $M2$ nature.

Since the BC crossing is not seen in the alignment plot, fig. 7, the AB neutrons are most likely involved in the configuration. A possible interpretation could therefore be $[404]7/2^+\otimes$AB describing the lower part of the band, which agrees with the new observed decay to the $[404]7/2^+$ band. Other possibilities such as $[402]5/2^+\otimes$AB or $[411]1/2^+\otimes$AB cannot immediately be excluded, yet the $[411]1/2^+\otimes$AB band would be expected to have a larger signature splitting. However, the $[404]7/2^+$ band has the lowest excitation energy at spins around the AB crossing and is more strongly populated. Therefore, the $[404]7/2^+\otimes$AB configuration seems to be the most obvious candidate. Note that the $[404]7/2^+$ band changes character above the apparent AB crossing as explained above.

A gain in alignment of $\sim 3\hbar$ is seen around $\hbar\omega \sim 0.38$ MeV. This suggests that a change of character occurs at this frequency in the X3 band, which is supported by the observation of a continuation, consisting of three levels reaching spin $63/2^+$, of the negative-signature partner of the configuration $[404]7/2^+\otimes$AB, see fig. 5. The upper part of band X3 resembles the behavior of the $[523]7/2^-\otimes$AEBC band with respect to excitation energy as a function of spin, fig. 5, but is located at a higher energy. It is therefore proposed that the top part of X3 can be assigned the configuration $[514]9/2^-\otimes$AEBC.

4.1.6 The band X4

The band X4 was found in the previous experiment [18]. Based on the striking similarity with the $[523]7/2^-\otimes$AEBC band in the alignment plot, fig. 7, the band was assigned the configuration $[523]7/2^-\otimes$AGBC. However, since the H neutron is predicted lower in energy than G by UC, we now prefer the configuration of band

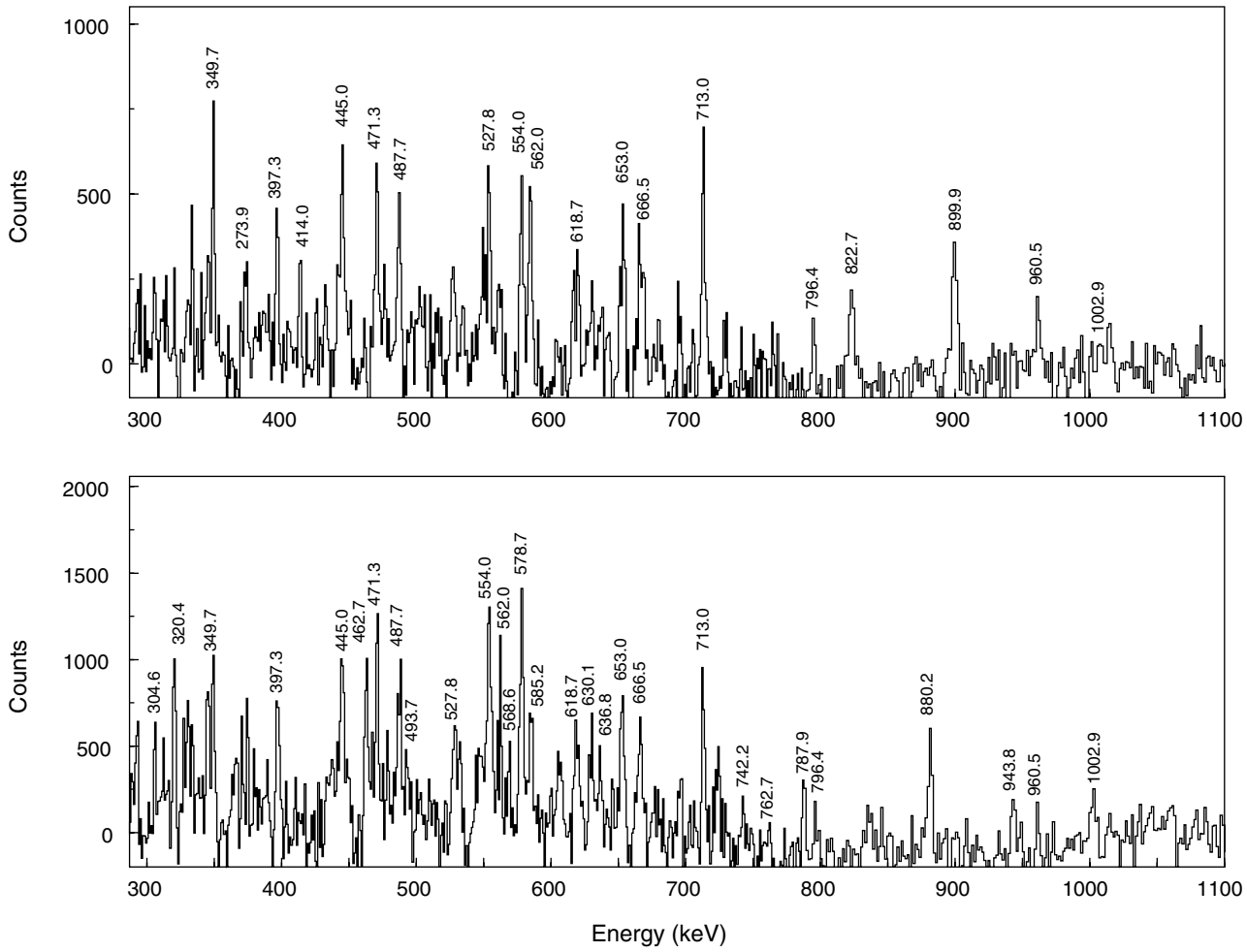

Fig. 9. Upper spectrum showing the ND band X3 obtained from the 3D-coincidence cube using a sum of double gates on the transitions 822.7, 414.0, 713.0 keV. The lower spectrum also shows the band X3 using a sum of double gates on the transitions 713.0, 787.9, 880.2, 943.8, 1002.9 keV.

X4 as $[523]7/2^-\otimes$AHBC. This also agrees very well with the excitation energy, which is ~ 250 keV larger than that of $[523]7/2^-\otimes$AEBC at spin $71/2\hbar$.

4.1.7 The band X5

The band X5, observed for the first time in the present experiment, is established up to spin $99/2\hbar$, which is the highest spin observed in any of the bands including the TSD bands, see fig. 10. At spin $75/2\hbar$ the band decays to the $[523]7/2^-\otimes$AB band through a 1015.0 keV transition. An angular distribution ratio, $W(25°)/W(90°) = 1.43\pm0.25$ and a polarization, $P = 0.11\pm0.03$ agree with a $\Delta I = 2$ $E2$ character for this transition, and X5 therefore has parity and signature $(\pi, \alpha) = (-, +1/2)$. The band X5 possesses a very large alignment, fig. 6, which indicates that one of the proton intruder orbitals, $h_{9/2}[541]1/2^-$ or $i_{13/2}[660]1/2^+$ is likely to be involved in the configuration. Both of these intruder orbitals have an expected large signature splitting in energy and the favoured signature is $\alpha = +1/2$ (cf. n and m in table 2).

To obtain $(\pi, \alpha) = (-, -1/2)$ as determined for X5 with $[541]1/2^-$ requires a change in signature. The possible quasiparticle combinations expected low in excitation energy are nefAC or nhfAB. In either case the band nefAB with $(\pi, \alpha) = (-, +1/2)$ is expected appreciably lower in energy. Such a band with equally large alignment which would most likely decay into the $\alpha = +1/2$ signature partner of the $[523]7/2^-\otimes$AB band has not been observed. Therefore, the $h_{9/2}[541]1/2^-$ orbital is not likely to be involved in the configuration of X5.

Alternatively, the configuration $i_{13/2}[660]1/2^+\otimes$AEBC with $(\pi, \alpha) = (-, -1/2)$, involving the same combination of quasineutrons which, coupled to the two signature partners of the negative-parity $[523]7/2^-$ proton orbital, becomes yrast in the spin interval $I \sim 28$–38, is suggested. The alignment difference between $[523]7/2^-\otimes$AEBC and X5 is about $5\hbar$ at $\hbar\omega \sim 0.5$ MeV, where X5 starts, which is consistent with the expected alignment difference between the $i_{13/2}[660]1/2$ and $h_{11/2}[523]7/2^-$ orbitals. The observed increase in alignment of X5 at $\hbar\omega \sim 0.5$-0.6 MeV would be explainable as caused by alignment of the first pair, ef, of $h_{11/2}$ quasiprotons. The observed features are

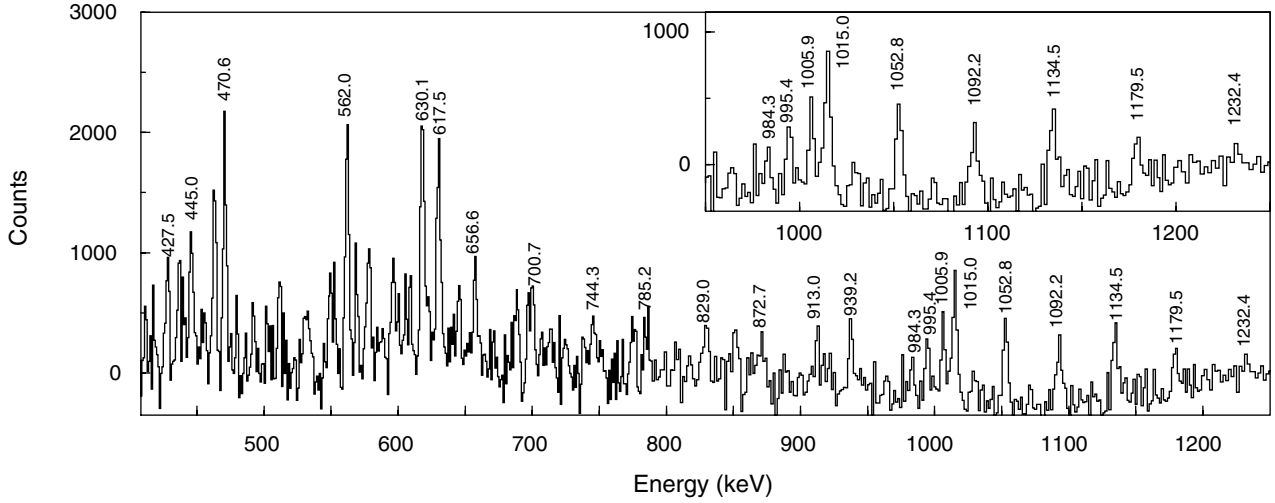

Fig. 10. Spectrum showing the ND band, X5, obtained from the 3D-coincidence cube using a sum of double gates on the transitions 1015.0, 1052.8, 1092.2, 1134.5, 1179.5, and 1232.4 keV. The inset shows an expansion of the high-energy part of the spectrum.

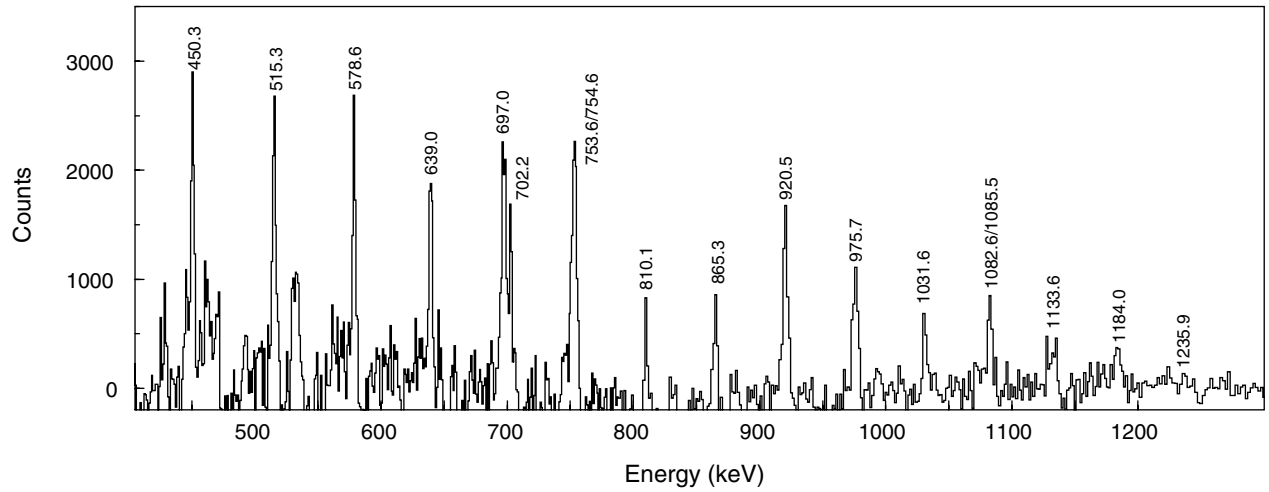

Fig. 11. Spectrum documenting TSD4 and the $\Delta I = 1$ decay-out transitions to TSD1 using a sum of double gates on 386.3, 450.3, 515.3, 578.6, 639.0, 697.0, 752.6 and 805.6 keV in TSD1 together with 810.1 and 865.3 keV in TSD4.

consistent with the configuration $i_{13/2}[660]1/2^+ \otimes$AEBC which is therefore considered a likely assignment of X5.

4.2 Triaxial strongly deformed structures

Four TSD bands, fig. 3, have been firmly established in ^{163}Lu and the two lowest excited bands, TSD2 and TSD3, have recently been assigned as a one- and two-phonon wobbling excitation, respectively, built on the yrast $\pi i_{13/2}$ TSD band, TSD1 [11,12]. Spin and parity of the three lowest bands, TSD1-3, have in this connection been uniquely determined. In the present experiment a fourth band, TSD4, first reported in ref. [18], has been observed to decay to TSD1 via four weakly populated transitions. In fig. 11 a spectrum of TSD4 is shown, where the four decay-out transitions of energies 1082.6, 1133.6, 1184.0 and 1235.9 keV, indicated tentatively in ref. [18], are now clearly seen. A spectrum of the decay-out transitions of TSD4, obtained from the filter matrix, is presented in fig. 12. The enhancement, achieved by applying the filtering technique, of especially the 1184.0 and 1235.9 keV γ-rays is striking. The populations of TSD1-4 relative to ND yrast are $\sim 10\%$, 3%, 1.2% and 0.9%, respectively.

4.2.1 Spin and parity assignment of TSD4

Angular distribution and DCO ratios have been obtained for some of the decay-out transitions of TSD4, see table 4. Unfortunately, these values do not provide definite information about the spin of TSD4, since they agree with both $\Delta I = 0$ pure $E2$ nature as well as $\Delta I = 1$ pure $E1$, $M1$ or $E2$ nature for the decay-out transitions, see fig. 1, disregarding transitions of $M2$ nature. In the case of $\Delta I = 0$ decay, transitions of $\Delta I = 2$ character are expected to compete in the decay due to the large transition energies of ~ 1880 keV. However, a search for these $\Delta I = 2$

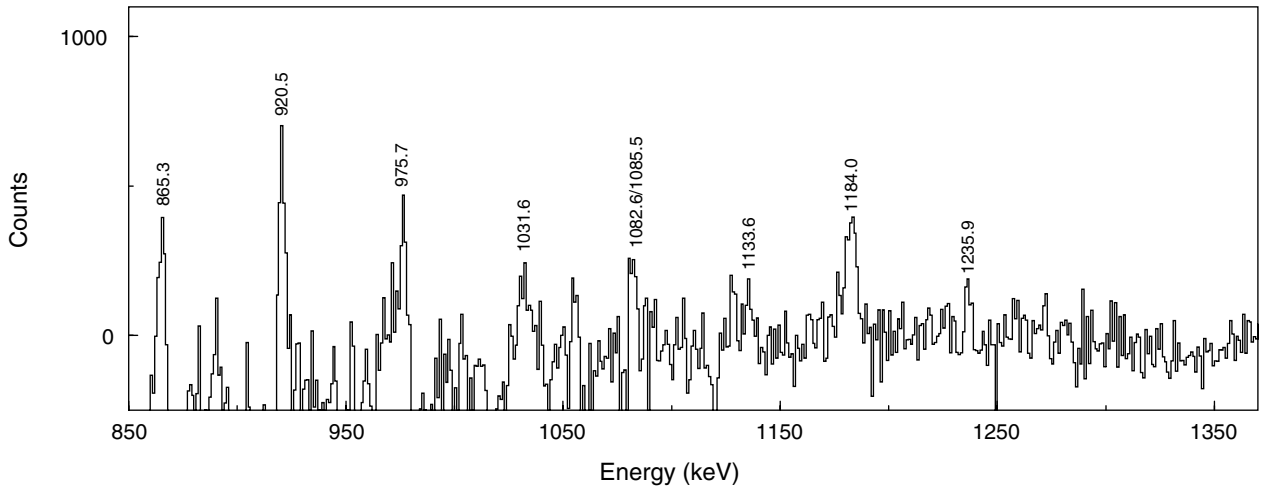

Fig. 12. Spectrum obtained from a filter matrix, filtered on transitions in TSD1, using a sum of single gates on the transitions 702.2, 810.1 and 865.3 keV in TSD4. The decay-out transitions to TSD1 are clearly identified.

Table 4. Experimental values of angular distribution ratio, $W(25°)/W(90°)$, DCO ratio, $R_{\rm DCO}$, for the $\Delta I = 1$ transitions from TSD4 to TSD1.

E_γ (keV)	$I_{\rm i}^\pi \rightarrow I_{\rm f}^\pi$	$\frac{W(25°)}{W(90°)}$	$R_{\rm DCO}$
1082.6	$\frac{59}{2}^{(-)} \rightarrow \frac{57}{2}^{+}$	0.71(13)	
1133.6	$\frac{55}{2}^{(-)} \rightarrow \frac{53}{2}^{+}$	0.75(22)	
1184.0	$\frac{51}{2}^{(-)} \rightarrow \frac{49}{2}^{+}$	0.66(20)	0.58(17)
1235.9	$\frac{47}{2}^{(-)} \rightarrow \frac{45}{2}^{+}$	0.70(21)	

transitions came out negative. The most likely solution is therefore $\Delta I = 1$ character for the decay-out transitions of TSD4, which means that TSD4 has signature $\alpha = -1/2$. This spin assignment also agrees well with the relative population of TSD4 compared to TSD3. In fig. 13 the excitation energy of TSD1-4 relative to a rigid-rotor reference is shown as a function of spin together with some of the ND bands for comparison. The parity of TSD4 is ambiguous, since a polarization measurement of the decay-out transitions was impossible due to low statistics.

4.2.2 Configuration assignment of TSD4

In contrast to TSD2-3, TSD4 cannot be interpreted in terms of the wobbling phonon picture, since the band possesses rotational properties different from those of TSD1-3. In fig. 14 the dynamic moments of inertia of the four TSD bands are shown as a function of rotational frequency. It is obvious that the nature of TSD4 is different from that of TSD1-3. In the frequency range between $\hbar\omega \sim 0.38$ MeV and $\hbar\omega \sim 0.5$ MeV TSD1-3 all have a bump, which is not seen in TSD4. It is suggested that this bump is related to a gradual alignment of the first pair of $i_{13/2}$ neutrons, which must be blocked in the configuration of TSD4. By taking this bump into account, the moment of inertia related to the core of the configurations of TSD1-3 may in fact be smaller than that of TSD4. With

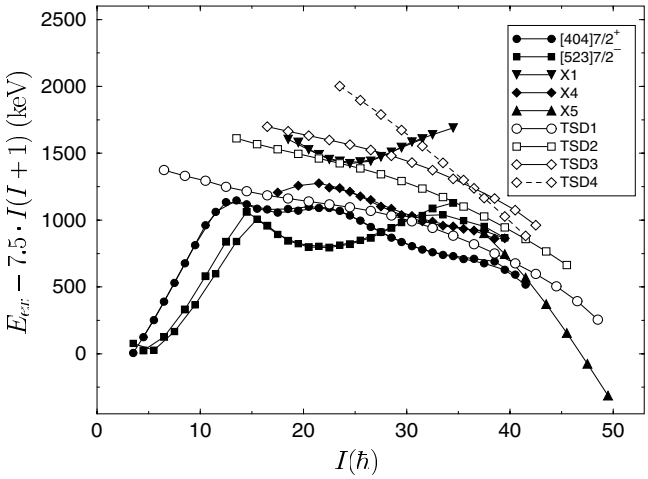

Fig. 13. Excitation energy relative to a rigid rotor as a function of spin for TSD1-4 together with some of the ND bands.

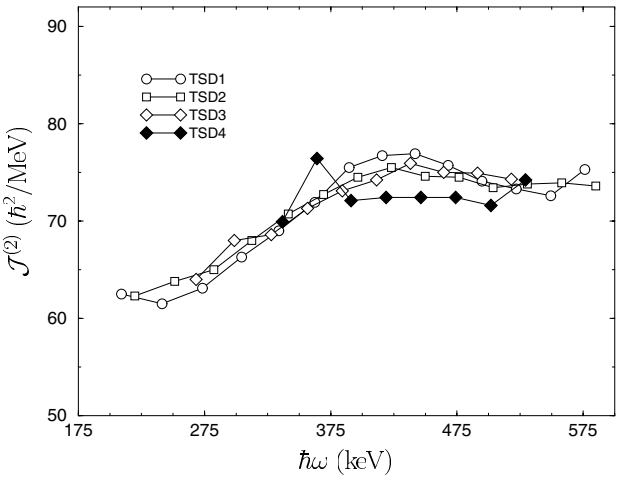

Fig. 14. Dynamic moments of inertia for TSD1-4 as a function of rotational frequency.

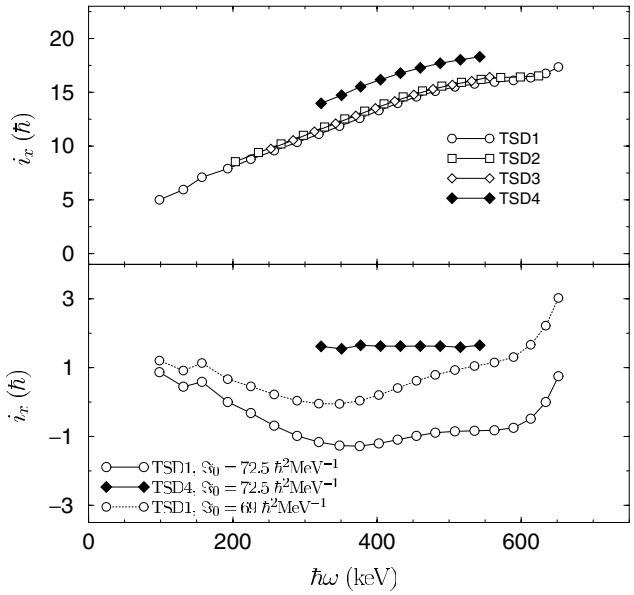

Fig. 15. Upper panel: Alignment of TSD1-4, as a function of rotational frequency, using a reference with $J_0 = 30\hbar^2$ MeV^{-1} and $J_1 = 40\hbar^4$ MeV^{-3}. Lower panel: Alignment of TSD4 and TSD1 using $J_0 = 72.5\hbar^2$ MeV^{-1} and $J_1 = 0$. For comparison the alignment of TSD1 is shown using $J_0 = 69\hbar^2$ MeV^{-1} and $J_1 = 0$.

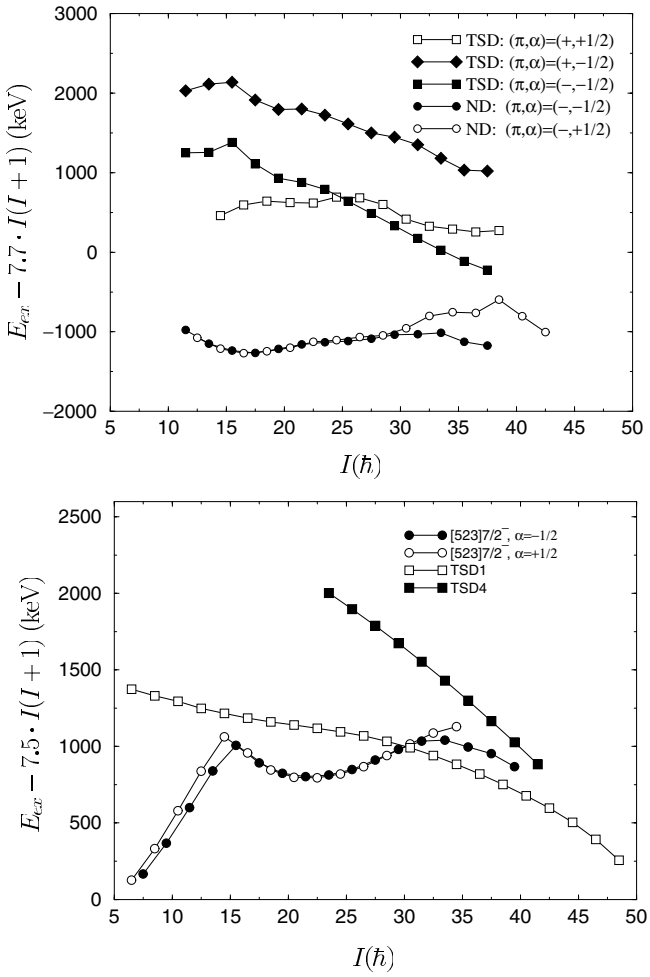

Fig. 16. Upper panel: calculated excitation energy relative to a rigid reference of the configurations matching the [523]7/2$^-\otimes$AB ND band and TSD1 as well as the two possible configurations of TSD4 using Ultimate Cranker. Lower panel: the corresponding experimental observations. Note that two different references have been used in the figures.

the configuration of TSD4 most likely based on the excitation of two quasineutrons in addition to a quasiproton, the neutron pairing will be reduced, which is consistent with the suggested larger moment of inertia in TSD4 compared to TSD1-3.

A question arises when analyzing the difference in relative alignments, $i_x = I_x - I_{\rm ref}$ of the TSD bands, where $I_{\rm ref}$ is supposed to express the projection of the collective angular momentum on the cranking axis following the commonly used cranking formulation for observed quantities. The alignment of TSD4 appears for a given $\hbar\omega$ to be $\sim 3\hbar$ larger than that of TSD1-3 when using a standard reference of $I_{\rm ref} = J_0\omega + J_1\omega^3$ with $J_0 = 30\hbar^2$ MeV^{-1} and $J_1 = 40\hbar^4$ MeV^{-3}, see fig. 15 (upper panel). This diference reduces to $\sim 2.2\hbar$ by applying the appropriate frequencies, $\hbar\omega_{\rm i}$ and $\hbar\omega_{\rm f}$ associated with the initial and final states, respectively, of the transitions from TSD4 to TSD1. By choosing instead a reference with $J_0 = 72.5\hbar^2$ MeV^{-1} and $J_1 = 0$, close to the observed, almost constant dynamic moment of inertia of TSD4, *i.e.* assuming that the angular momentum is almost fully collective, an alignment difference of $\sim 3\hbar$, independent of frequency in the relevant frequency range is obtained, as illustrated in the lower panel of fig. 15. Such large alignment differences make the suggested $\Delta I = 1$ $E1$ decay of TSD4 unlikely, since a dipole transition cannot carry more than $1\hbar$ of angular momentum. However, as discussed above, the moments of inertia of the cores of TSD1-3 are smaller than that of TSD4, which suggests the use of different references when comparing the alignments. To show the sensitivity of the alignment difference to the choice of references, the alignment of TSD1 is pictured in the lower panel of fig. 15, also using a rigid reference with a smaller value of $J_0 = 69\hbar^2$ MeV^{-1}. Surprisingly, $\sim 5\%$ reduction in the value of J_0 for TSD1 is sufficient to change the apparent alignment difference between TSD4 and TSD1 from $\sim 3\hbar$ to $\sim 1\hbar$, which would be in agreement with the $\Delta I = 1$ dipole decay of TSD4. Of course, a fully rigid reference moment of inertia is unrealistic, and the present analysis therefore only qualitative, but indicative of the properties of the two bands allowing the dipole decay between them.

Since TSD4 exhibits properties quite different from TSD2-3, which have been assigned as wobbling excitations based on a comparison with particle rotor calculations, it is likely that TSD4 can be interpreted in terms of usual quasiparticle excitations calculated with UC. In addition to the $\pi i_{13/2}$ assignment to TSD1 other examples of TSD bands assigned with configurations based on UC calculations are $\pi i_{13/2}\nu h_{9/2}$ and $\pi i_{13/2}\nu i_{13/2}$ for TSD1 and TSD3 in ^{164}Lu [22]. We refer here to the main component of l_j as calculated in a stretched basis [23]. It should also be mentioned that the wobbling solutions do not emerge from the principal axis cranking calculations. In fig. 16 (upper

panel) the calculated excitation energies relative to a rigid-rotor reference of the two lowest possible configurations of TSD4 with $(\pi,\alpha)=(+,-1/2)$ and $(\pi,\alpha)=(-,-1/2)$ are shown together with those of the configurations of TSD1 and the ND band $[523]7/2^{-}\otimes$AB. In these calculations the neutron pairing for the two candidate bands for TSD4 is reduced to ~ 0.47 MeV compared with 0.6 MeV for the configuration of TSD1 at $I = 30$–$35\hbar$. In the lower panel of fig. 16 the corresponding experimental observations are pictured. First of all, it should be noted that, in general, the UC does not reproduce the observed energy difference between the TSD and ND configurations very well, whereas the relative excitation between individual TSD (and ND) configurations may be more reliable. The configuration with $(\pi,\alpha)=(-,-1/2)$ is close to the $(\pi,\alpha)=(+,+1/2)$ configuration (TSD1) and it becomes yrast above spin $25\hbar$, *i.e.* it is the lowest configuration in the calculations taking all combinations of parity and signature into account. The calculated alignment for the proposed configuration of TSD4 relative to that calculated for TSD1 varies from about $+2$ to $-2\hbar$ in the frequency range $0.40 \leq \hbar\omega \leq 0.55$ MeV, which does not agree with observations, but here the AB neutron crossing whose interaction strength is found to be very shape dependent may be the cause of this discrepancy. The other possible solution for TSD4, $(\pi,\alpha)=(+,-1/2)$, is located at a much higher excitation energy. We therefore propose that TSD4 most likely is a $(\pi,\alpha)=(-,-1/2)$ band. In terms of quasiparticles this configuration corresponds to a$\otimes$BF. That is, the lowest $i_{13/2}$ quasiproton coupled to the two lowest quasineutrons ($i_{13/2}$ and $h_{9/2}$) with $(\pi,\alpha)=(+,-1/2)$ and $(\pi,\alpha)=(-,-1/2)$, respectively, which are the same neutron orbitals as suggested in ^{164}Lu for TSD3 and TSD1. Note that the labelling of the quasiparticles in this case has no resemblance to that of the quasiparticles entering in the ND configurations. Experimentally TSD4 is not observed to become yrast around spin $25\hbar$, but the overall agreement between experiment and theory illustrated in fig. 16 is fairly good.

From the measured branching ratios, and the assumption of a Q_t for the in-band $E2$ transitions of $\sim 9b$, an average value of $B(E1) \sim 1.3 \cdot 10^{-3} e^2$ fm^2 for the four $\Delta I = 1$ decay-out transitions of TSD4 may be estimated, which also supports the assignment of TSD4 as a negative-parity band. The extracted $B(E1)$ value is rather large, but is not unreasonable taking the possibility for an enhancement due to an admixture of octupole vibrations into account. Comparable $B(E1)$ values have recently been measured for transitions connecting the SD6 band in ^{152}Dy [24], interpreted as a rotational band built on a collective octupole vibration, to the SD1 band. On the other hand, the extracted average values of $B(M1) \sim 0.13\mu_N^2$ or $B(E2)_{\rm out}/B(E2)_{\rm in} \sim 0.05$, assuming positive parity of TSD4, are much larger than expected for the signature partner of TSD1 or a 3-quasiparticle configuration. The $B(M1)$ value is approximately a factor of 10 too large and also the large $B(E2)_{\rm out}/B(E2)_{\rm in}$ value would be difficult to explain. We therefore prefer to assign negative parity to TSD4. As mentioned above, the bump observed in the dynamic moments of inertia for TSD1-3 is most likely related to a gradual alignment of the AB neutrons, see fig. 14. In TSD4, the bump is not observed agreeing very well with the assignment of TSD4 as the a$\otimes$BF band, in which the AB alignment is blocked. The measured average $B(E1)$ value for the TSD4 $\rightarrow$ TSD1 transitions may then have their origin mostly in the admixted $f_{7/2}$ amplitude in the negative-parity quasineutron for which the main component is $h_{9/2}$, which together with the $i_{13/2}$ quasineutron may be responsible for coupling to octupole vibrational degrees of freedom. In this connection some caution should be taken with respect to a detailed comparison of TSD4 with the UC calculations.

5 Discussion

Shape coexistence between ND and TSD structures is a well-established phenomenon among nuclei belonging to the $A \sim 165$ mass region. The present ND level scheme of ^{163}Lu provides together with the four TSD bands, TSD1-4, an additional example of the shape coexistence predicted by the UC calculations. However, for the first time a band with different rotational properties, decaying into the yrast TSD band, has been observed within the TSD potential well of a nucleus. The assignment of TSD4 in ^{163}Lu as a three-quasiparticle excitation, in addition to the discovery of the one- and two-phonon wobbling excitations, illustrates the richness of rotational modes available to a triaxial nucleus. The wobbling excitations observed in ^{163}Lu are energetically favoured by the triaxial deformation of the nuclear system and the fully aligned $i_{13/2}$ proton [16,17], and they therefore appear low in energy. However, rotational bands which can be interpreted as quasiparticle excitations in the principal axis cranking description, such as the TSD bands observed in ^{164}Lu [22], may still be expected to coexist with the wobbling excitations. The present understanding of the nature of TSD4 supports this expectation.

In a count fluctuation analysis [25] of the ridge structures, formed by unresolved rotational bands, in 2D spectra obtained from the previous data set, it was found that more than 40 bands could exist in the TSD potential well of ^{163}Lu and 20 bands in the ND well [26]. Besides the four firmly established TSD bands additionally three TSD bands, presumably belonging to ^{163}Lu, have been observed in the present experiment, which is in agreement with the predictions from the count fluctuation analysis. The three TSD bands could not be connected to ND states due to low statistics. In ref. [26], it was also concluded that at lower excitation energy, near TSD yrast, a substantial potential barrier separates the ND and TSD wells. Therefore, at intermediate spin crosstalk through the barrier between ND and TSD states is not expected. This prediction is in fact observed experimentally in the present discrete line analysis. In fig. 13 it is seen that even though the TSD states of TSD1-4 at several spin values come close to the ND states, no transitions have been observed between the involved states from the two potential wells. This is in contrast to the situation in ^{167}Lu, where the

TSD1 band is observed to interact with an ND band at spin $61/2\hbar$ indicating that the barrier in ^{167}Lu is less pronounced compared to ^{163}Lu [14]. Another interesting observation is that the ND band, X5, is yrast above spin $83/2\hbar$. This is indeed surprising since this means that the ND and TSD states coexist even at the highest spins. The observation of the band, X5, has also shown that a multi-quasiparticle ND band, probably involving the intruder orbital $\pi i_{13/2}[660]1/2^+$, has a lower excitation energy than the states of TSD1 at high spin.

The positive-parity ND bands show a remarkable systematic behaviour, see fig. 5. The lowest configuration at high spin is $[523]7/2^-\otimes$AEBC, and the next configuration, $[523]7/2^-\otimes$AHBC (band X4), is located ~ 250 keV higher in energy at spin $71/2\hbar$, corresponding roughly to the expected energy difference between the H and E quasineutrons. The second $h_{11/2}$ proton orbital $[514]9/2^-$ is expected about 500 keV higher in excitation energy than $[523]7/2^-$, and the assignment of $[514]9/2^-\otimes$AEBC to band X3 agrees very well with the general systematics for the positive-parity ND bands. In addition, it appears that the positive-parity band $[523]7/2^-\otimes$AE involving the negative-parity AE two-quasineutrons with the BC crossing unblocked is lower in excitation energy than the negative-parity band with configuration $[523]7/2^-\otimes$AB above spin $\sim 55/2\hbar$, where the band $[523]7/2^-\otimes$AEBC actually becomes yrast, until crossed by X5 at spin $\sim 83/2\hbar$, see figs. 4 and 5.

It should also be noted that the $[541]1/2^-$ band is not observed in ^{163}Lu in contrast to ^{165,167}Lu, where this band is well established [27,28]. This is in agreement with the UC calculations, which predict the $[541]1/2^-$ orbital to be located at higher energy in ^{163}Lu due to the smaller deformation compared to ^{165}Lu and ^{167}Lu.

The proposed involment of the $\pi i_{13/2}$ orbital in the configuration of a new normal deformed band with a very large alignment is particularly interesting since it would trace this orbital at two different equlibrium deformations, $(\varepsilon,\gamma) =\sim (0.27, 0^\circ)$ and $(\varepsilon,\gamma) =\sim (0.39, 20^\circ)$ as expected for the normal deformed and for the triaxial strongly deformed well, respectively, for this orbital.

6 Summary and conclusion

The nucleus ^{163}Lu has been investigated extensively through a series of experiments during the last few years [11,12,29] and the large number of observed bands related to different shapes of the nucleus has provided a unique possibility for studying coexistence, not only between ND and TSD structures, but also between different rotational structures within the TSD potential well of ^{163}Lu.

In a search for a two-phonon wobbling excitation using the Euroball array, a third excited band, TSD4, has been observed in addition to the two lower excited TSD bands, TSD2-3, assigned as one- and two-phonon wobbling excitations, respectively, built on the yrast $\pi i_{13/2}$ band, TSD1. Four decay-out transitions presumably of $\Delta I = 1$ $E1$ character have been found connecting TSD4 to TSD1. The band, TSD4, shows rotational properties different from those of TSD1-3, and can therefore not be interpreted in terms of the wobbling phonon picture. Instead, the lowest configurations calculated by the Ultimate Cranker (UC) code have been investigated in an attempt to explain TSD4 in terms of quasiparticle excitations. It is proposed that TSD4 can be interpreted as a negative-parity band built on the same quasiproton as the yrast band, TSD1, coupled to the two lowest $h_{9/2}$ and $i_{13/2}$ quasineutrons of negative and positive parity, respectively.

The ND level scheme of ^{163}Lu has been extended to high spin, and a total of eight coupled bands and one single band has been firmly established and configurations of the various bands have been proposed. The ND level scheme provides, together with the four TSD bands, an example of shape coexistence between ND and TSD rotational structures. Furthermore, for the first time rotational structures of different nature have been identified within the TDS potential well of a nucleus. The present observation of coexisting quasiparticle and wobbling excitations in the TSD potential well of ^{163}Lu provides yet a new example of the rich variety of rotational excitations available to a triaxial nucleus.

This research is supported by the Danish Science Foundation, the EU, Contract No. HPRI-CT-1999-00078 and BMBF, Germany, contract No. 06 BN 907. The A. von Humboldt foundation is also acknowledged.

References

1. I. Ragnarsson, Phys. Rev. Lett. **62**, 2084 (1989).
2. G. Andersson, Nucl. Phys. A **268**, 205 (1976).
3. T. Bengtsson, Nucl. Phys. A **496**, 56 (1989); **512**, 124 (1990).
4. R. Bengtsson, `www.matfys.lth.se/~ragnar/ultimate.html`.
5. G.B. Hagemann, *Wobbling phonon excitations in strongly deformed triaxial nuclei*, to be published in Eur. Phys. J. A.
6. W. Schmitz, H. Hübel, C.X. Yang, G. Baldsiefen, U. Birkental, G. Frölingsdorf, D. Mehta, R. Müßeler, M. Neffgen, P. Willsau, G.B. Hagemann, A. Maj, D. Müller, J. Nyberg, M. Piiparinen, A. Virtanen, R. Wyss, Phys. Lett. B **303**, 230 (1993).
7. G. Schönwaßer, H. Hübel, G.B. Hagemann, J. Domscheit, A. Görgen, B. Herskind, G. Sletten, D.R. Napoli, C. Rossi-Alvarez, D. Bazzacco, R. Bengtsson, P.O. Tjöm, S.W. Ødegård, Eur. Phys. J. A **13**, 291 (2002).
8. G. Schönwaßer, H. Hübel, G.B. Hagemann, H. Amro, R.M. Clark, M. Cromaz, R.M. Diamond, P. Fallon, B. Herskind, G. Lane, W.C. Ma, A.O. Macchiavelli, S.W. Ødegård, G. Sletten, D. Ward, J.N. Wilson, Eur. Phys. J. A **15**, 435 (2002).
9. A. Görgen *et al.*, to be published.
10. H. Amro, P.G. Varmette, W.C. Ma, B. Herskind, G.B. Hagemann, G. Sletten, R.V.F. Janssens, M. Bergström, A. Bracco, M. Carpenter, J. Domscheit, S. Frattini, D.J. Hartley, H. Hübel, T.L. Khoo, F. Kondev, T. Lauritsen, C.J. Lister, B. Million, S.W. Ødegård, R.B. Piercey, L.L. Riedinger, K.A. Schmidt, S. Siem, I. Wiedenhöver, J.N. Wilson, J.A. Winger, Phys. Lett. B **506**, 39 (2001).

11. S.W. Ødegård, G.B. Hagemann, D.R. Jensen, M. Bergström, B. Herskind, G. Sletten, S. Törmänen, J.N. Wilson, P.O. Tjøm, I. Hamamoto, K. Spohr, H. Hübel, A. Görgen, G. Schönwasser, A. Bracco, S. Leoni, A. Maj, C.M. Petrache, P. Bednarczyk, D. Curien, Phys. Rev. Lett. **86**, 5866 (2001).
12. D.R. Jensen, G.B. Hagemann, I. Hamamoto, S.W. Ødegård, B. Herskind, G. Sletten, J.N. Wilson, K. Spohr, H. Hübel, P. Bringel, A. Neußer, G. Schönwaßer, A.K. Singh, W.C. Ma, H. Amro, A. Bracco, S. Leoni, G. Benzoni, A. Maj, C.M. Petrache, G. Lo Bianco, P. Bednarczyk, D. Curien, Phys. Rev. Lett. **89**, 142503 (2002).
13. G. Schönwaßer, H. Hübel, G.B. Hagemann, P. Bednarczyk, G. Benzoni, G. Lo Bianco, A. Bracco, P. Bringel, R. Chapman, D. Curien, J. Domscheit, B. Herskind, D.R. Jensen, S. Leoni, W.C. Ma, A. Maj, A. Neußer, S.W. Ødegård, C.M. Petrache, D. Roßbach, H. Ryde, K.H. Spohr, A.K. Singh, Phys. Lett. B **552**, 9 (2003).
14. H. Amro, W.C. Ma, G.B. Hagemann, B. Herskind, G. Sletten, J.N. Wilson, D.R. Jensen, J. Thompson, J.A. Winger, P. Fallon, D. Ward, R.M. Diamond, A. Görgen, A.O. Macchiavelli, H. Hübel, J. Domscheit, I. Wiedenhöver, Phys. Lett. B **553**, 197 (2003).
15. P. Bringel *et al.*, to be published.
16. I. Hamamoto, Phys. Rev. C **65**, 044305 (2002).
17. I. Hamamoto, G.B. Hagemann, Phys. Rev. C **67**, 014319 (2003).
18. D.R. Jensen, G.B. Hagemann, I. Hamamoto, S.W. Ødegård, M. Bergström, B. Herskind, G. Sletten, S. Törmänen, J.N. Wilson, P.O. Tjøm, K. Spohr, H. Hübel, A. Görgen, G. Schönwasser, A. Bracco, S. Leoni, A. Maj, C.M. Petrache, P. Bednarczyk, D. Curien, Nucl. Phys. A **703**, 3 (2002).
19. J. Simpson, Z. Phys. A **358**, 139 (1997).
20. D.C. Radford, Nucl. Instrum. Methods A **361**, 297 (1995).
21. J.N. Wilson, B. Herskind, Nucl. Instrum. Methods A **455**, 612 (2000).
22. S. Törmänen, S.W. Ødegård, G.B. Hagemann, A. Harsmann, M. Bergström, R.A. Bark, B. Herskind, G. Sletten, P.O. Tjøm, A. Görgen, H. Hübel, B. Aengenvoort, U.J. van Severen, C. Fahlander, D. Napoli, S. Lenzi, C. Petrache, C. Ur, H.J. Jensen, H. Ryde, R. Bengtsson, A. Bracco, S. Frattini, R. Chapman, D.M. Cullen, S.L. King, Phys. Lett. B **454**, 8 (1999).
23. H. Schnack-Petersen, R. Bengtsson, R.A. Bark, P. Bosetti, A. Brockstedt, H. Carlsson, L.P. Ekström, G.B. Hagemann, B. Herskind, F. Ingebretsen, H.J. Jensen, S. Leoni, A. Nordlund, H. Ryde, P.O. Tjöm, C.X. Yang, Nucl. Phys. A **594**, 175 (1995).
24. T. Lauritsen, R.V.F. Janssens, M.P. Carpenter, P. Fallon, B. Herskind, D.G. Jenkins, T.L. Khoo, F.G. Kondev, A. Lopez-Martens, A.O. Macchiavelli, D. Ward, K. Abu Saleem, I. Ahmed, R.M. Clark, M. Cromaz, T. Døssing, A.M. Heinz, A. Korichi, G. Lane, C.J. Lister, D. Seweryniak, Phys. Rev. Lett. **89**, 282501 (2002).
25. T. Døssing, B. Herskind, S. Leoni, A. Bracco, R.A. Broglia, M. Matsuo, E. Vigezzi, Phys. Rep. **268**, 1 (1996).
26. S.W. Ødegård, B. Herskind, T. Døssing, G.B. Hagemann, D.R. Jensen, G. Sletten, J.N. Wilson, S. Leoni, P.O. Tjøm, P. Bednarczyk, D. Curien, Eur. Phys. J. A **14**, 309 (2002).
27. G. Schönwaßer, N. Nenott, H. Hübel, G.B. Hagemann, P. Bednarczyk, G. Benzoni, G. Lo Bianco, A. Bracco, P. Bringel, R. Chapman, D. Curien, J. Domscheit, B. Herskind, D.R. Jensen, S. Leoni, W.C. Ma, A. Maj, A. Neußer, S.W. Ødegård, C.M. Petrache, D. Roßbach, H. Ryde, K.H. Spohr, A.K. Singh, to be published.
28. D. Roux *et al.*, to be published.
29. J. Domscheit, S. Törmänen, B. Aengenvoort, H. Hübel, R.A. Bark, M. Bergström, A. Bracco, R. Chapman, D.M. Cullen, C. Fahlander, S. Frattini, A. Görgen, G.B. Hagemann, A. Harsmann, B. Herskind, H.J. Jensen, S.L. King, S. Lenzi, S.W. Ødegård, C.M. Petrache, H. Ryde, U.J. van Severen, G. Sletten, P.O. Tjøm, C. Ur, Nucl. Phys. A **660**, 381 (1999).